Available online at www.sciencedirect.com
SciVerse ScienceDirect
Procedia Engineering 56 (2013) 217 – 224
Procedia Engineering
www.elsevier.com/locate/procedia

5th BSME International Conference on Thermal Engineering

Effects of curvature on unsteady solutions through a curved square duct flow

Md. Saidul Islam[a]* and Rabindra Nath Mondal[b]

[a] *Mathematics Discipline; Science, Engineering and Technology School, Khulna University, Khulna-9208, Bangladesh*
[b] *Department. of Mathematics, Faculty of Science, Jagannath University, Dhaka-1100, Bangladesh*

Abstract

The present study addresses numerical prediction of fully developed two-dimensional laminar flow of viscous incompressible fluid through a curved square duct with curvature ranging from 0.001 to 0.5. Numerical calculations are carried out over a wide range of the Dean number $0 < Dn \leq 6000$ with a temperature difference between the vertical sidewalls for the Grashof number Gr = 1000, where the outer wall is heated and the inner wall cooled. Spectral method is used as a basic tool to solve the system of non-linear differential equations. First, we investigated steady solutions by using Newton-Raphson iterations method. As a result, a complex structure of steady solutions with two- and multi-vortex solutions is obtained. Then, in order to investigate the non-linear behavior of the unsteady solutions, time evaluations calculations are performed and the transition between two types of solutions is determined by drawing the phase spaces of the time evolution solutions. It is found that the unsteady flow undergoes in the scenario '*steady-state* → *periodic* → *multi-periodic* → *chaotic*, if the Dean number is increased no matter what the curvature is. Secondary flow patterns, axial flow distribution and temperature profiles on the flow characteristics are also obtained.

Keywords: Curved square duct; secondary flow; unsteady solutions; Dean number; time evolution

Nomenclature

Dn	: Dean number	T	: Temperature
g	: Gravitational acceleration	u	: Velocity components in the $x-$direction
Gr	: Grashof number	v	: Velocity components in the $y-$direction
h	: Half height of the cross section	w	: Velocity components in the $z-$direction
d	: Half width of the cross section	x	: Horizontal axis
L	: Radius of the curvature	y	: Vertical axis
P_r	: Prandtl number	z	: Axis in the direction of the main flow
t	: Time	λ	: Resistance coefficient

Greek letters

δ	: Curvature of the duct	υ	: Kinematic viscosity
ρ	: Density	κ	: Thermal diffusivity
ψ	: Sectional stream function	μ	: Viscosity

* Corresponding author. Tel.: +88-01710851580; Fax: +88-02-7113752.
E-mail address: rnmondal71@yahoo.com

doi:10.1016/j.proeng.2013.03.110

1. Introduction

The study of flows and heat transfer through curved ducts and channels has been and continues to be an area of paramount interest of many researchers because of the diversity of their practical applications in fluids engineering, such as in fluid transportation, turbo machinery, refrigeration, air conditioning systems, heat exchangers, ventilators, centrifugal pumps, internal combustion engines and blade-to-blade passage for cooling system in modern gas turbines. The flow through curved a duct shows physically interesting features under the action of centrifugal force caused by the curvature of the duct. The presence of curvature produces centrifugal forces which acts at right angle to the main flow direction and creates secondary flows. Dean [1] was the first who formulated the problem in mathematical terms under the fully developed flow conditions and showed the existence of a pair of counter rotating vortices in a curved pipe. The readers are referred to Berger *et al*. [2], Nandakumar and Masliyah [3] and Yanase *et al.* [4] for some outstanding reviews on curved duct flows.

Considering the non-linear nature of the Navier-Stokes equation, the existence of multiple solutions does not come as a surprise. The solution structure of fully developed flow is commonly present in a bifurcation diagram which consists of a number of lines (branches) connecting different possible solutions. These branches can bifurcate and show multiple solutions in limit points (Mondal, [5]). An early complete bifurcation study of two-dimensional flow through a curved duct of square cross section was conducted by Winters [6]. Wang and Yang [7] performed numerical as well as experimental investigations of periodic oscillations for the fully developed flow in a curved square duct. Unsteady flow characteristics through a curved rectangular duct were investigated in detail by Yanase *et al*. [8]. Recently, Mondal *et al*. [9] performed comprehensive numerical study on fully developed bifurcation structure and stability of two-dimensional (2D) flow through a curved duct with square cross section and found a close relationship between the unsteady solutions and the bifurcation diagram of steady solutions. The flow through a curved duct with differentially heated vertical sidewalls has another aspect because secondary flows promote fluid mixing and heat transfer in the fluid. Recently, Mondal *et al*. [10] performed numerical investigations of non-isothermal flows through a curved duct with square cross section, where they studied the flow characteristics with the effects of secondary flows on convective heat transfer.

In the present study, a numerical result is presented for the fully developed two-dimensional flow of viscous incompressible fluid through a curved square duct with various curvatures. Investigating effect of curvature on unsteady solutions is an important objective of the present study.

2. Mathematical formulations

Consider an incompressible viscous fluid streaming through a curved duct with square cross section whose width or height is 2*d*. The coordinate system with the relevant notations is shown in Fig. 1. It is assumed that the outer wall of the duct is heated while the inner one cooled. The temperature of the outer wall is $T_0 + \Delta T$ and that of the inner wall is $T_0 - \Delta T$, where $\Delta T > 0$. The x, y and z axes are taken to be in the horizontal, vertical, and axial directions, respectively. It is assumed that the flow is uniform in the axial direction, and that it is driven by a constant pressure gradient G along the center-line of the duct, i.e. the main flow in the axial direction as shown in Fig. 1. The variables are non-dimensionalized by using the representative length d and the representative velocity $U_0 = \nu/d$. We introduce the non-dimensional variables defined as

$$u = \frac{u'}{U_0}, \qquad v = \frac{v'}{U_0}, \quad w = \frac{\sqrt{2\delta}}{U_0} w', \quad x = \frac{x'}{d}, \quad \bar{y} = \frac{y'}{d}, \quad z = \frac{z'}{d}$$

$$T = \frac{T'}{\Delta T}, \quad t = \frac{U_0}{d} t', \quad \delta = \frac{d}{L}, \quad P = \frac{P'}{\rho U_0^2}, \; G = \frac{\partial P'}{\partial z'} \frac{d}{\rho U_o{}^2}$$

where u, v, and w are the non-dimensional velocity components in the x, y, and z directions, respectively; t is the non-dimensional time, P the non-dimensional pressure, δ the non-dimensional curvature, and temperature is non-dimensionalized by ΔT. Henceforth, all the variables are nondimensionalized, if not specified.

The sectional stream function ψ is introduced as

$$u = \frac{1}{1+\delta x} \frac{\partial \psi}{\partial \bar{y}}, \; v = -\frac{1}{1+\delta x} \frac{\partial \psi}{\partial x}. \tag{1}$$

Then the basic equations for w, ψ and T are derived from the Navier-Stokes equations and the energy equation under the *Boussinesq approximation* as,

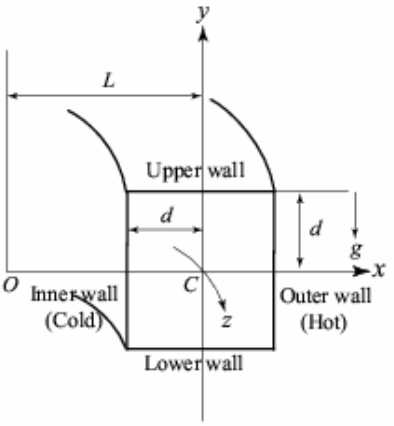

Fig. 1. Coordinate system of the curved duct

$$(1+\delta x)\frac{\partial w}{\partial t}+\frac{\partial(w,\psi)}{\partial(x,y)}-D_n+\frac{\delta^2 w}{1+\delta x}=(1+\delta x)\Delta_2 w-\frac{\delta}{(1+\delta x)}\frac{\partial\psi}{\partial y}w+\delta\frac{\partial w}{\partial x} \tag{2}$$

$$\left(\Delta_2-\frac{\delta}{1+\delta x}\frac{\partial}{\partial x}\right)\frac{\partial\psi}{\partial t}=-\frac{1}{(1+\delta x)}\frac{\partial(\Delta_2\psi,\psi)}{\partial(x,y)}+\frac{\delta}{(1+\delta x)^2}\times\left[\frac{\partial\psi}{\partial y}\left(2\Delta_2\psi-\frac{3\delta}{1+\delta x}\frac{\partial\psi}{\partial x}+\frac{\partial^2\psi}{\partial x^2}\right)-\frac{\partial\psi}{\partial x}\frac{\partial^2\psi}{\partial x\partial y}\right]+\frac{\delta}{(1+\delta x)^2}$$
$$\times\left[3\delta\frac{\delta^2\psi}{\partial x^2}-\frac{3\delta^2}{1+\delta x}\frac{\partial\psi}{\partial x}\right]-\frac{2\delta}{1+\delta x}\frac{\partial}{\partial x}\Delta_2\psi+w\frac{\partial w}{\partial y}\times\Delta_2^2\psi-Gr(1+\delta x)\frac{\partial T}{\partial x}, \tag{3}$$

$$\frac{\partial T}{\partial t}+\frac{1}{(1+\delta x)}\frac{\partial(T,\psi)}{\partial(x,y)}=\frac{1}{\mathrm{Pr}}\left(\Delta_2 T+\frac{\delta}{1+\delta x}\frac{\partial T}{\partial x}\right). \tag{4}$$

where

$$\Delta_2\equiv\frac{\partial^2}{\partial x^2}+\frac{\partial^2}{\partial y^2},\quad \frac{\partial(f,g)}{\partial(x,y)}\equiv\frac{\partial f}{\partial x}\frac{\partial g}{\partial y}-\frac{\partial f}{\partial y}\frac{\partial g}{\partial x}. \tag{5}$$

The Dean number D_n, the Grashof number G_r, and the Prandtl number P_r, which appear in Eqs. (2) to (4) are defined as

$$D_n=\frac{Gd^3}{\mu\nu}\sqrt{\frac{2d}{L}},\quad G_r=\frac{\beta g\Delta T d^3}{\nu^2},\quad P_r=\frac{\nu}{k} \tag{6}$$

where μ,ν,k and g are the viscosity, the coefficient of thermal expansion, the coefficient of thermal diffusivity and the gravitational acceleration respectively.

The rigid boundary conditions for w and ψ are used as

$$w(\pm1,y)=w(x,\pm1)=\psi(\pm1,y)=\psi(x,\pm1)=\frac{\partial\psi}{\partial x}(\pm1,y)=\frac{\partial\psi}{\partial y}(x,\pm1)=0 \tag{7}$$

and the temperature T is assumed to be constant on the walls as

$$T(1,y)=1,\ T(-1,y)=-1,\ T(x,\pm1)=x\,. \tag{8}$$

The upper and lower walls are adiabatic. In the present study, *Dn* and δ are varied while *Gr* and *Pr* are fixed as Gr = 1000 and *Pr* = 7.0 (water).

3. Method of numerical calculation

In order to obtain the numerical solutions, spectral method is used. The main objective of the method is to use the expansion of the polynomial functions that is the variables are expanded in the series of functions consisting of Chebyshev polynomials. The expansion function $\phi_n(x)$ and $\psi_n(x)$ are expressed as

$$\Phi_n(x)=\left(1-x^2\right)C_n(x),\ \Psi_n(x)=\left(1-x^2\right)^2 C_n(x), \tag{9}$$

where $C_n(x) = \cos(n\cos^{-1}(x))$ is the n^{th} order Chebyshev polynomial. $w(x,y,z)$, $\psi(x,y,t)$ and $T(x,y,t)$ are expanded in terms of $\Phi_n(x)$ and $\Psi_n(x)$ as

$$\left.\begin{aligned} w(x,y,z) &= \sum_{m=0}^{M}\sum_{n=0}^{N} w_{mn}(t)\Phi_m(x)\Phi_n(y), \\ \psi(x,y,t) &= \sum_{m=0}^{M}\sum_{n=0}^{N} \psi_{mn}(t)\Psi_m(x)\Psi_n(y), \\ T(x,y,t) &= \sum_{m=0}^{M}\sum_{n=0}^{N} T_{mn}(t)\Phi_m(x)\Phi_n(y) + x, \end{aligned}\right\} \tag{10}$$

where M and N are the truncation numbers in the x and y directions respectively. The expansion coefficients w_{mn}, ψ_{mn} and T_{mn} are then substituted into the basic Eqs. (2), (3) and (4) and the collocation method is applied. As a result, the nonlinear algebraic equations for w_{mn}, ψ_{mn} and T_{mn} are obtained. The collocation points are taken to be

$$\left.\begin{aligned} x_i &= \cos\left[\pi\left(1-\frac{i}{M+2}\right)\right], \quad i = 1,...,M+1, \\ y_i &= \cos\left[\pi\left(1-\frac{i}{N+2}\right)\right], \quad j = 1,...,N+1. \end{aligned}\right\} \tag{11}$$

where $i = 1,...,M+1$ and $j = 1,...,N+1$. In the present study, numerical calculations are carried out over a wide range of the Dean number $0 < Dn \le 6000$ and the Grashof number $Gr = 1000$ for the square duct of curvatures ranging from $\delta = 0.001$ to $\delta = 0.3$. For sufficient accuracy of the solutions, we used M = 20 and N = 20. Steady solutions are obtained by the Newton-Raphson iteration method. Finally, to calculate the unsteady solutions, Crank-Nicolson and Adams-Bashforth methods together with the function expansion and collocation methods are applied to the equations (2) to (4).

4. Resistance coefficient

We use the resistance coefficient λ as one of the representative quantities of the flow state. It is also called the *hydraulic resistance coefficient*, and is generally used in fluids engineering, defined as

$$\frac{P_1^* - P_2^*}{\Delta z^*} = \frac{\lambda}{dh^*}\frac{1}{2}\rho\left\langle w^* \right\rangle^2, \tag{12}$$

where quantities with an P_1^* be asterisk denote dimensional ones, $\langle\ \rangle$ stands for the mean over the cross section of the duct and $d_h^* = 4(2d \times 2dl)/(4d + 4dl)$ is the hydraulic diameter. The main axial velocity $\langle w^* \rangle$ is calculated by

$$\langle \omega^* \rangle = \frac{v}{4\sqrt{2\delta d}} \int_{-1}^{1} dx \int_{-1}^{1} \omega(x,y,t)dy \tag{13}$$

Here, λ is related to the mean non-dimensional axial velocity $\langle \omega \rangle$ as

$$\lambda = \frac{4\sqrt{2\delta}Dn}{\langle \omega \rangle^2} \tag{14}$$

where $\langle w \rangle = \sqrt{2\delta}d / v\left\langle w^* \right\rangle$. In this paper, λ is used to find the solution structure of the steady solutions and to find the unsteady solutions by numerical computations.

5. Results and discussion

5.1 *Steady solutions*

With the present numerical calculation, we obtain a single but entangled branch of steady solution for $Gr = 1000$ over the Dean number $0 < Dn \le 6000$. To obtain the steady solution, we used path continuation technique as discussed by Mondal [5]. The solution structure of the steady solution is shown in Fig 2(a). An enlargement of Fig. 2(a) is also shown in Fig. 2(b). It is found that the branch starts from point a ($Dn \approx 0$) and goes to the direction of increasing Dn and

decreasing λ up to point b ($Dn = 4823$), where it experiences a smooth turning and goes to the direction of increasing λ and decreasing Dn up to point c ($Dn = 3897$). At point c, the branch experiences another interesting turning and goes to the direction of increasing Dn and decreasing λ up to point d ($Dn = 4976$), where the branch turns very smoothly and goes to the direction of increasing λ and decreasing Dn up to point e ($Dn = 3862$) and then to point f ($Dn = 4156$), and finally extents to increasing Dn through points g and h. It is found that the branch consists of asymmetric two- and four-vortex solutions, which are not shown here for brevity.

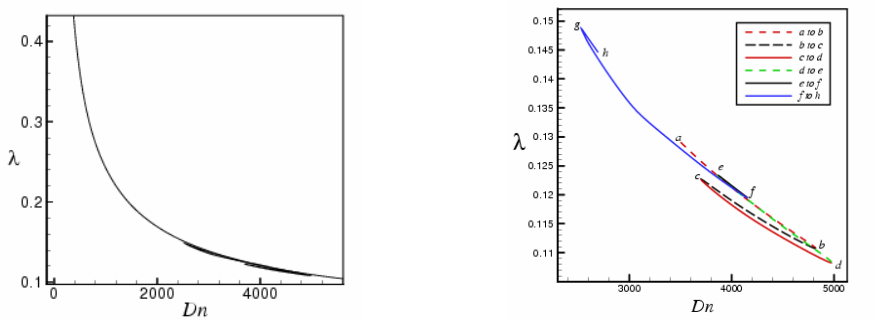

(a) (b)

Fig. 2. (a) Solution structure of the steady solution for $Gr = 1000$ and $0 < Dn \le Dn \le 5500$ at $\delta = 0.1$
(b) An enlargement of Fig. 2(a) at $1180 \le Dn \le 5200$.

5.2 *Time evolution of the unsteady solutions*

In order to study the non-linear behavior of the unsteady solutions, we perform time-evolution calculations of λ at various *Dn* for the curvatures ranging from $\delta = 0.001$ to $\delta = 0.3$ for *Gr* =1000. However, in this section, we only show the results of unsteady solutions for the curvature $\delta = 0.1$, and complete unsteady solutions ranging from $\delta = 0.001$ to $\delta = 0.3$, are shown in a phase diagram in the next section.

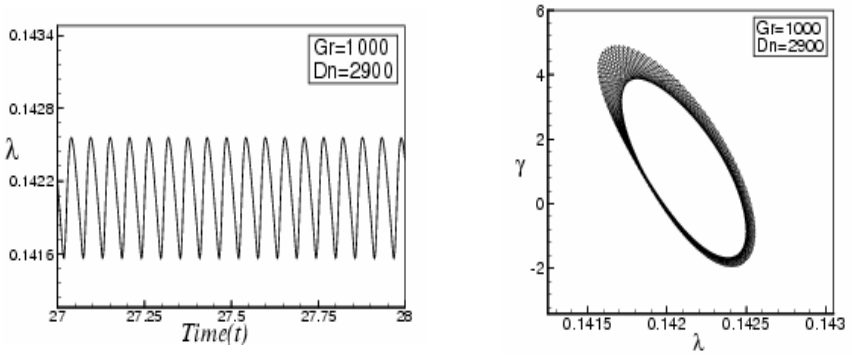

(a) (b)

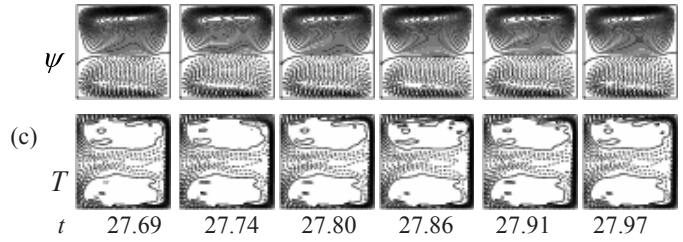

Fig. 3. (a) Time evolution of λ for $Dn = 2900$ and $Gr = 1000$ at $\delta = 0.1$ (b) Phase space of the time evolution of λ for $Dn = 2900$ and $Gr = 1000$ (c) Contours of secondary flow patterns (top) and temperature profile (bottom) for one period of oscillation at time $27.69 \le t \le 27.97$.

To investigate the non-linear behavior of unsteady solutions, we studied time evolution of λ for $Dn = 2900$ and $Gr = 1000$ at $\delta = 0.1$ as shown in Fig. 3(a). Figure 3(a) shows that the unsteady flow at $Dn = 2900$ is a periodic solution, which is well justified by drawing a phase spaces as shown in Fig. 3(b). We also show typical contours of secondary flow patterns and temperature profiles, for one period of oscillation at time $27.69 \le t \le 27.97$, in Fig. 3(c). It is found that the unsteady solution at $Dn = 2900$ and $Gr = 1000$ at $\delta = 0.1$ is an asymmetric two-vortex solution. Then, we studied the time evolution of λ for $Dn = 2925$ as shown in Fig. 4(a). It is found that the unsteady flow at $Dn = 2925$ is a multi-periodic oscillation. In order to observe the multi-periodic solution more clearly, we draw the phase space as shown in Fig. 4(b). In order to view the change of the flow characteristics as time proceeds, typical contours of secondary flow patterns and temperature profiles are shown in Fig. 4(c). It is found that the unsteady solution at $Dn = 2925$ and $Gr = 1000$ is an asymmetric two-vortex solution. We studied the time evolution of λ for $Dn = 3000$ as shown in Fig. 5(a). It is found that the flow at $Dn = 3000$ is a transitional chaos, which is well justified by drawing the phase space as shown in Fig. 5(b). Then we obtained typical contours of secondary flow patterns and temperature profiles as shown in Fig. 5(c). It is found that the chaotic oscillation at $Dn = 3000$ and $Gr = 1000$ is an asymmetric two-vortex solution.

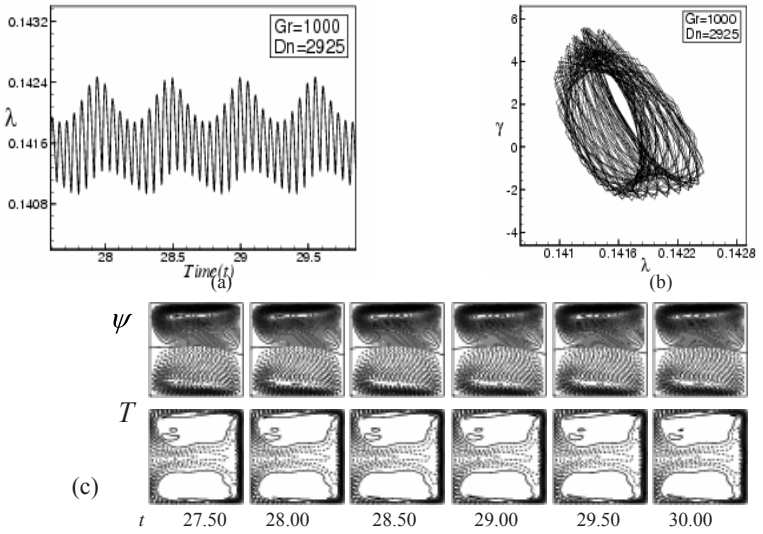

Fig. 4. (a) Time evolution of λ for $Dn = 2925$ and $Gr = 1000$ at $\delta = 0.1$ (b) Phase space of the time evolution of λ for $Dn = 2925$ (c) Contours of secondary flow patterns (top) and temperature profiles (bottom) for $Dn = 2925$ and $Gr = 1000$ at time $27.50 \le t \le 30.00$.

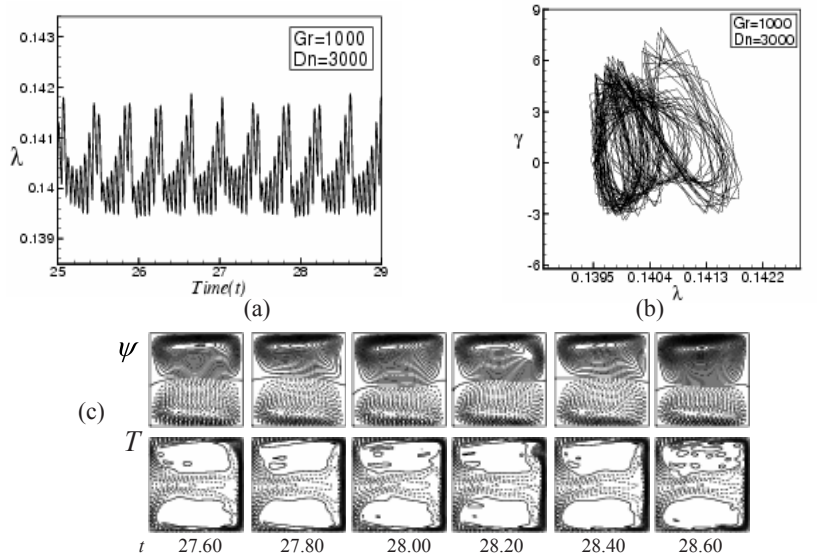

Fig. 5. (a) Time evolution of λ for $Dn = 3000$ and $Gr = 1000$ (b) Phase space of the time evolution of λ for $Dn = 3000$ (c) Contours of secondary flow patterns (top) and temperature profiles (bottom) for $Dn = 3000$ and $Gr = 1000$ at time $27.60 \le t \le 28.60$.

It is found that the unsteady solution at $Dn = 3450$ and $Gr = 1000$ is an asymmetric two-vortex solution. We studied the time evolution of λ for $Dn = 3450$ as shown in Fig. 6(a). It is found that the flow at $Dn = 3450$ is a transitional chaos, which is well justified by drawing the phase space as shown in Fig. 6(b). Then we obtained typical contours of secondary flow patterns and temperature profiles as shown in Fig. 6(c). It is found that the chaotic oscillation at $Dn = 3450$ and $Gr = 1000$ is an asymmetric two-vortex solution.

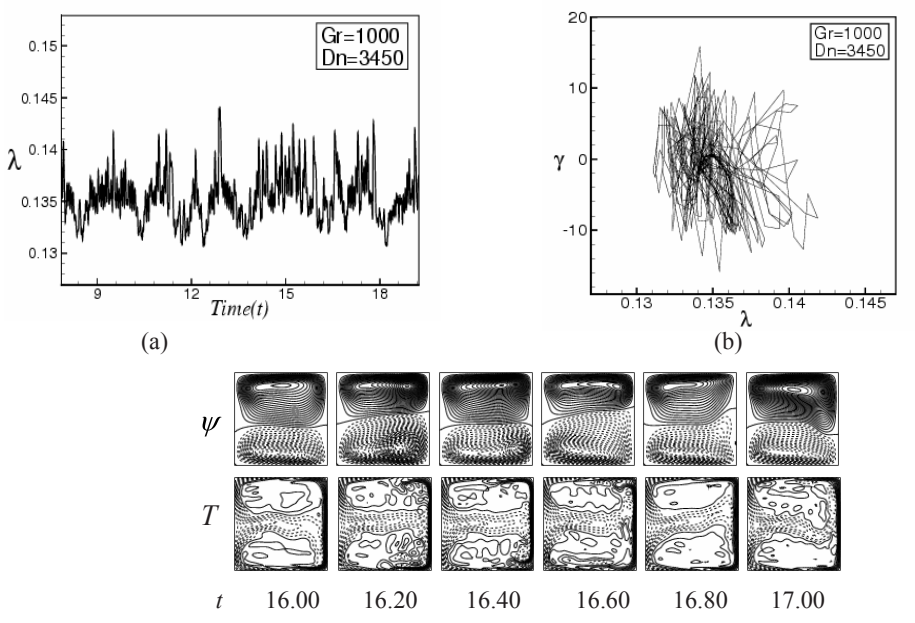

Fig. 6. (a) Time evolution of λ for $Dn = 3450$ and $Gr = 1000$ (b) Phase space of the time evolution of λ for $Dn = 3450$ (c) Contours of secondary flow patterns (top) and temperature profiles (bottom) for $Dn = 3450$ and $Gr = 1000$ at time $16.00 \le t \le 17.00$.

5.3 *Phase diagram in the $Dn - \delta$ plane*

Here, the complete unsteady solutions, obtained by the time evolution computations in the present study, are shown by a phase diagram in Fig. 6 in the $Dn - \delta$ plane for $0 < Dn \le 6000$ and $0.001 \le \delta \le 0.5$ for $Gr = 1000$. In this figure, the circles indicate steady-state solutions, crosses periodic solutions and triangles chaotic solutions. As seen in Fig. 6, the steady-state solution turns into chaotic solution through periodic or multi-periodic oscillation if Dn is increased, no matter what the curvature is.

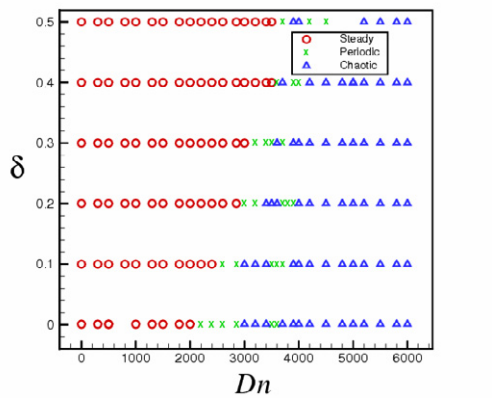

Fig. 7. Distribution of the unsteady solutions in the $Dn - \delta$ plane for $0 < Dn \le 6000$ and curvature $0.001 \le \delta \le 0.5$ for $Gr = 1000$ (o: steady-state solution, ×: periodic solution and △: chaotic solution).

6. Conclusion

A comprehensive numerical study is presented for the flow characteristics through a curved square duct. Numerical calculations are carried out by using a spectral method and covering a wide range of the Dean numbers $0 < Dn \le 6000$ and the curvature $0.001 \le \delta \le 0.5$ for the Grashof number $Gr = 1000$. First a single branch of asymmetric steady solution is obtained with two- and four-vortex solution. Then, in order to investigate the non-linear behavior of the unsteady solutions, time evaluation calculations as well as their phase space are performed. It is found that the flow becomes steady-state for $Dn < 2900$ but periodic at $Dn = 2900$, multi-periodic solutions for $2925 \le Dn < 3000$ and chaotic solutions for $3000 \le Dn \le 3450$. Thus the unsteady flow undergoes in the scenario "*steady* $\rightarrow$ *periodic* $\rightarrow$ *multi-periodic* $\rightarrow$ *chaotic*", if Dn is increased up to 3450. If the Dean number is increased further, that is, for $Dn > 3450$ the unsteady flow undergoes through various flow instabilities in the scenario "*periodic* $\rightarrow$ *multi-periodic* $\rightarrow$ *chaotic* $\rightarrow$ *periodic* $\rightarrow$ *chaotic*", if Dn is increased. Secondary flow patterns and temperature profiles are also obtained and it is found that the secondary flow is a two-vortex solution for the unsteady solution.

Acknowledgement

Md Saidul Islam, one of the authors, would like to gratefully acknowledge and express his deepest gratitude and thanks to the Ministry of Science & Technology (MOST) for awarding him a research fellowship (No.39.012.002.01.30.014.2010-237/45) for master's program in session 2010-2011.

References

[1] Dean, W. R. (1927). Note on the motion of fluid in a curved pipe. *Phil. Mag.* Vol. **4**(20), pp. 208- 223.

[2] Berger, S.A., Talbot, L., Yao, L. S. (1983). Flow in Curved Pipes, *Annual. Rev. Fluid. Mech*., Vol. **35**, pp. 461-512.

[3] Nandakumar, K. and Masliyah, J. H. (1986). Swirling Flow and Heat Transfer in Coiled and Twisted Pipes, *Adv. Transport Process*., Vol. **4**, pp. 49-112.

[4] Yanase, S., Kaga, Y. and Daikai, R. (2002). Laminar flow through a curved rectangular duct over a wide range of the aspect ratio, *Fluid Dynamics Research*, Vol. **31,** pp. 151-183.

[5] Mondal, R. N. (2006). Isothermal and Non-isothermal Flows Through Curved ducts with Square and Rectangular Cross Sections, *Ph.D. Thesis*, Department of Mechanical Engineering, Okayama University, Japan.

[6] Winters, K. H., 1987. A bifurcation study of laminar flow in a curved tube of rectangular cross-section, *J. Fluid Mech.* Vol. **180**, pp. 343--369.

[7] Wang, L. and Yang, T., 2005. Periodic oscillation in curved duct flows, *Physica D*, Vol. **200**, pp. 296—302

[8] Yanase, S, Mondal, R. N. and Kaga, Y. (2005). Numerical study of non-isothermal flow with convective heat transfer in a curved rectangular duct, *International Journal of Thermal Sciences*, Vol. **44** (11), pp. 1047-1060.

[9] Mondal, R. N., Kaga, Y., Hyakutake, T.and Yanase, S. (2007). Bifurcation Diagram for Two- dimensional Steady Flow and Unsteady Solutions in a Curved Square Duct, *Fluid Dynamics Research*. Vol. **39**, pp. 413-446.\

[10] Mondal, R. N., Uddin, M. S. and Yanase, S. (2010). Numerical prediction of non-isothermal flow through a curved square duct, *Int. J. Fluid Mech. Research*, Vol. **37(1)**, pp. 85-99.